



Contents lists available at ScienceDirect

Advanced Powder Technology

journal homepage: www.elsevier.com/locate/apt

Original Research Paper

Development of compartmentalized antibacterial systems based on encapsulated alliinase

L. Mašková^a, P. Janská^a, V. Klimša^a, Z. Knejzlík^{a,b}, V. Tokárová^a, O. Kašpar^{a,*}^a Department of Chemical Engineering, University of Chemistry and Technology Prague, Technická 5, 166 28 Prague 6, Czech Republic^b Institute of Organic Chemistry and Biochemistry of the Czech Academy of Sciences, Flemingovo náměstí 2, 166 10 Prague 6, Czech Republic

ARTICLE INFO

Article history:

Received 19 January 2021

Received in revised form 15 May 2021

Accepted 22 May 2021

Available online xxx

Keywords:

Alliinase

Encapsulation

Spray-drying

Allicin

Antibacterial activity

ABSTRACT

Alliin, an organic compound produced via the transformation of biologically inactive alliin by alliinase, an enzyme found in garlic, combines a strong antibacterial effect with suppressed development of bacterial resistance. However, because of the high reactivity and volatility, controlled *in-situ* production of alliin that mimics the natural synthesis is essential to achieve desired therapeutic effects. In this work, the spray-drying technique was employed for encapsulation of alliinase into polymer micro-carriers with an emphasis on the effect of process parameters, i.e., drying temperature, nozzle type, choice of the carrier materials, on the activity of encapsulated alliinase in soluble maltodextrin and swellable chitosan microparticles. The results show that maltodextrin is a suitable carrier for the effective protection of alliinase against thermal stress. On the other hand, we can control alliin production and release from chitosan carriers with immobilized alliinase by variation of the cross-linker amount. Antibacterial activity of *in-situ* formed alliin vapors was confirmed against *Escherichia coli* bacterial strain using customized sample holders preventing physical contact of powder sample with the inoculated agar plate.

© 2021 The Society of Powder Technology Japan. Published by Elsevier BV and The Society of Powder Technology Japan. All rights reserved.

1. Introduction

An increasing number of multidrug-resistant (MDR) bacterial strains hand-in-hand with the fact that only a few new antibiotics have been discovered during the past 30 years (known as the discovery void) [1] were identified as a major threat to modern global society. Less than 100 years after the breakthrough discovery of penicillin [2], we are facing the grim scenario that even common superficial injuries or routine surgical procedures may become dangerous and life-threatening again [3] and alternative solutions are, therefore, needed [4,5]. Recently, a new antibiotic (Halicin) was discovered by a novel methodology using AI machine learning and deep neural network for the prediction of antibacterial activity of molecules cataloged in enormous chemical libraries [6]. However, due to practical and financial difficulties associated with the development of new antibiotics, most pharmaceutical companies have already shifted their attention to other, more cost-effective products. On the other hand, we can find a variety of antibacterial substances in nature providing essential antibacterial protection for various living species for thousands of years. It has been reported that the development of bacterial resistance against

potent but highly reactive and unstable plant-specific bactericides found in genus *Allium* is more than 1000 times slower compared to certain antibiotics [7], which could be the key to drug sustainability.

Garlic (*Allium sativum*), one of the most studied plants in our history, has been used since ancient times all around the globe as a natural remedy praised for its healing powers. The substance responsible for the beneficial properties is one of the most bioactive compounds found in nature - alliin. Alliin is a volatile organosulfur low molecular weight compound with a short half-life produced upon mechanical damage of the garlic tissues. It is formed rapidly (greater than 97% conversion after 30 sec [8]) by the transformation of a non-proteinogenic amino acid alliin (a major organosulfur compound located in the cytoplasm) with the enzyme alliinase (isolated in the vacuoles) [9]. First, allyl sulfenic acid is formed in the presence of water and cofactor pyridoxal 5'-phosphate (PLP), followed by rapid condensation of two molecules to alliin (Fig. 1). Alliin, a substance found in a garlic cell, is not the only sulfoxide involved in the natural self-defense mechanism of genus *Allium* since other plants (e.g., onion, leek) have their chemical analogs, e.g., isoalliin, methiin, propiin and others (Fig. 1) [10]. The plant-specific compounds with similar chemical backbone share reaction mechanisms and produce corresponding thiosulfinates upon contact with alliinase [11].

* Corresponding author.

E-mail address: kasparo@vscht.cz (O. Kašpar).

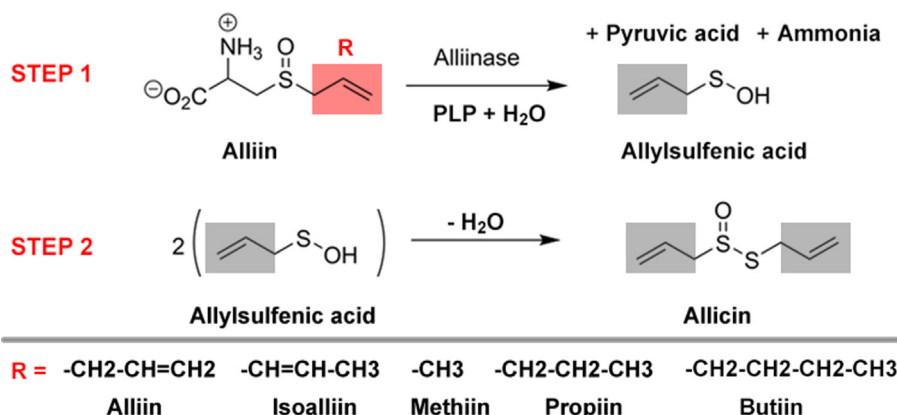


Fig. 1. Enzymatic conversion of alliin and alliin analogs.

Alliin volatility, high reactivity and short shelf-life are why the most effective way of alliin production is to mimic the original concept of a garlic cell compartmentalization, i.e., a binary system containing physically separated enzyme and substrate(s). Most commercial dietary products use powdered garlic where the enzyme, substrate and other compounds initially present in garlic are in the form of a dry powder [8]. Alliin as a prodrug has been declared by the FDA as a safe substance (GRAS - Generally Recognized As Safe), and it can be administered in unlimited amounts [12]. The most typical oral administration relies on rehydration and activation of the dry enzyme in an aqueous environment, e.g., saliva, gastric fluids, followed by the fast conversion of alliin into allicin. However, the acidic environment of gastric fluid and the action of digestive enzymes both result in complete deactivation of the unprotected enzyme, and only a minor fraction of the claimed allicin content is formed [13]. Several techniques have been employed for the improvement of alliinase stability and activity under various conditions along with the simplification of enzyme recovery and reuse, e.g., *i*) enzyme bonding through amino groups of lysine residues to sepharose and beaded cellulose [14]; *ii*) sugar-lectin binding to porous aluminum oxide [15]; *iii*) immobilization in layered double hydroxides [16]; *iv*) encapsulation into cross-linked polymers (alginate particles [16,17] and N-succinyl-chitosan [18]). Except for allicin synthesis, the immobilized alliinase can be valuable for biosensor development, e.g., detection of cysteine sulfoxides in food products [19].

To this date, the spray-drying technique, commonly used in the food and pharmaceutical industry for the encapsulation and drying of heat-sensitive materials such as probiotics [20], enzymes [21], monoclonal antibodies [22], or vitamins [23], has been used for encapsulation of alliinase only occasionally. For instance, Strehlow et al. demonstrated a successful encapsulation of alliinase in soluble lactose microparticles aimed at pulmonary delivery [24]. Allicin was formed upon rapid dissolution and mixing of two types of carriers (one with enzyme and the other one with alliin) in the alveolar model.

In this work, spray-dryer Büchi B-290 was employed for the preparation of maltodextrin and cross-linked chitosan microparticles with alliinase with controllable swelling aimed to control alliin production. Maltodextrin is a popular encapsulating agent for its low price, high water solubility, and low viscosity, which is in favor of the atomization and spray formation [25]. It has also been reported that maltodextrin, as wall material, provides effective protection of encapsulated proteins against external factors, i.e., oxidation and thermal stress [26]. The second carrier material, chitosan, belongs to the most commonly used compounds for microencapsulation thanks to being widely available, non-toxic, bioadhesive, and biodegradable [27]. Moreover, in combination

with a suitable cross-linker, it allows encapsulation and protection of sensitive substances such as proteins in reusable insoluble carriers [21].

To the best of our knowledge, little is known about the relations between chitosan composition, matrix density and swelling behavior, the activity of the encapsulated alliinase, and mass transport of alliin/allicin, which are valuable information to *i*) control otherwise very fast enzymatic reaction; *ii*) prevent the burst release of allicin from compartmentalized systems; *iii*) tailor the release profile to the specific end-user application.

2. Materials and methods

2.1. Materials

Maltodextrin (dextrose equivalent 4.0–7.0), chitosan (low molecular weight; 75–85% deacetylated), pyridoxal 5'-phosphate hydrate (PLP; $\geq 98\%$ purity), Brilliant Blue G 250, ethylenediaminetetraacetic acid (EDTA; BioUltra; anhydrous; $\geq 99\%$ purity), Polyethylene glycol (PEG) 6000, kanamycin sulfate, and N-[Tris(hydroxymethyl)methyl]glycine (Tricine; $\geq 99\%$ purity) were purchased from Sigma-Aldrich (Germany). Bovine Serum Albumin (BSA; fraction V; pH 7.0; standard grade; lyophilized) was purchased from Serva Electrophoresis (Germany). Ethanol (absolute for UV spectroscopy), acetic acid (99% p.a.), concentrated phosphoric acid (85%), glycerol (anhydrous, p.a.), sodium phosphate dibasic heptahydrate, sodium phosphate monobasic dodecahydrate, Tryptone (microbiologically tested, peptone from casein), yeast extract, sodium chloride (p.a.), sodium hydroxide and potassium hydroxide were purchased from Penta Chemicals. Sodium tripolyphosphate (TPP; for analysis) was purchased from Acros Organics (part of Thermo Fisher Scientific, USA). L-lactate dehydrogenase (LDH) from rabbit muscle and nicotinamide adenine dinucleotide disodium salt grade II (NADH; purity $\sim 98\%$) were purchased from Roche Diagnostics (Switzerland). Demineralized water was produced by Aqual 25 (Czech Republic; conductivity $\sim 0.07 \mu\text{S}\cdot\text{cm}^{-1}$). All chemicals were used as received without any further purification. Garlic bulbs of Czech origin were purchased from a local market. *Escherichia coli* K12 (EC43) was kindly provided by Dr. Zdeněk Knejzlík (Czech Academy of Sciences).

2.2. Alliin synthesis

Alliin, a natural substrate for alliinase, was synthesized by a two-step method previously published by Stoll and Seebeck [28]. In the first step, L-cysteine (50 g; $0.413 \text{ mol}\cdot\text{dm}^{-3}$) was dissolved in 1.2 dm^3 of an aqueous solution of ammonium hydroxide

(2 mol.dm⁻³) and alkylated with allyl bromide (75.0 g; 0.620 mmol.dm⁻³) at 0 °C. After 40 min, the reaction was terminated, and volume reduced using a rotary evaporator. The raw product (S-(2-propenyl)cysteine) was filtered, washed with ethanol, vacuum dried, and recrystallized from 2:3 water/ethanol mixture. In the second step, S-(2-propenyl)cysteine (53.0 g; 0.329 mmol.dm⁻³) was suspended in 530 cm³ of water at 25 °C and mixed with hydrogen peroxide (30% w/w; 37 cm³) while stirring. After two days, the volume was reduced by a rotary evaporator, 400 cm³ of acetone was added, and the mixture was stirred for 2 h. Then, the crude (±)-L-Alliin was filtered, washed with 5:1 acetone/water mixture and vacuum dried. The product was used without additional separation of diastereomers.

2.3. Alliinase extraction

Alliinase was extracted from fresh garlic according to previously published protocols with minor modifications [29,30]. The whole isolation procedure was carried out at 4 °C. Peeled garlic cloves were homogenized using a hand mixer in a stabilizing buffer (ratio 1:1.5 w/v, pH 6.5, sodium phosphate buffer 0.02 mol.dm⁻³, glycerol 10% v/v, 5 mmol.dm⁻³ EDTA, NaCl 5% w/v, 0.02 mmol.dm⁻³ PLP). The garlic pulp mixture was squeezed through four layers of cheesecloth and further separated by vacuum filtration. Polyethylene glycol (PEG) 6000 (25% w/w) was added to the supernatant while stirring to ensure alliinase precipitation. After 30 min, the mixture was centrifuged (30 000 g, 30 min) and the obtained yellow pellet was resuspended in PLP solution (0.02 mmol.dm⁻³) followed by the second centrifugation cycle. The resulting supernatant containing alliinase was passed through a 0.45 µm syringe filter to remove residual solid impurities. The final solution was lyophilized and stored at -20 °C prior to use. The alliinase content in the lyophilized product was determined by the Bradford method for protein quantification using bovine serum albumin (BSA) as a standard according to the protocols described elsewhere [31–33].

2.4. Preparation of carrier solutions

Maltodextrin and chitosan were chosen as suitable carrier materials for the alliinase immobilization. Maltodextrin 3% w/w solution (labeled as A) was prepared by dissolving maltodextrin in demineralized water. Chitosan solution (labeled as B) was prepared by dissolving an appropriate amount of chitosan in an aqueous solution of acetic acid (1% v/v) under constant stirring at 1400 rpm and elevated temperature (60 °C). A corresponding amount of sodium tripolyphosphate (TPP) dissolved in 10 cm³ of the acetic acid solution was then added drop-wise to chitosan solution using a syringe (29Gx1/2", 0.33x12 mm) and left stirring (1400 rpm; 25 °C) overnight. TPP cross-linked carriers were prepared using 0.5% chitosan solution due to the formation of insoluble coagulates at higher chitosan concentrations (Table 1). Rheological properties of prepared chitosan solutions, i.e., viscosity

and surface tension, governing the morphological properties of a spray-dried powder, were determined by rotary viscosimeter Rheolab QC (Anton Paar). Surface tension measurements were performed on Attension Theta Optical Tensiometer (Biolin Scientific) using a pendant drop method coupled with image analysis.

2.5. Spray-drying process

All feed solutions were prepared as a mixture of a carrier solution (98 cm³) and alliinase or alliin (the appropriate amount to obtain 2% w/w powder product dissolved in 2 cm³ of Tricine-KOH buffer, 0.2 mol.dm⁻³, pH 8.0 ± 0.05). Feed solution, stirred at 1400 rpm, was directly spray-dried to prevent excessive enzyme degradation in an aqueous medium, which was slightly acidic in the case of chitosan solution.

Büchi Mini Spray-Dryer B-290 (Fig. 2A) was used for all experiments using filtered air as a drying medium (open mode configuration) and a high-performance cyclone for more efficient product separation. Two-fluid (2F) and ultrasonic (US) nozzles were used for feed atomization (Fig. 2B). Atomization via 2F nozzle relies on the atomization of a coherent inlet feed with the compressed air flowing through the nozzle (flow rate 473 dm³.hr⁻¹). US nozzle uses mechanical vibrations of the nozzle surface for droplet formation and it should, therefore, allow drying of materials sensitive to shear stress such as proteins [34]. The flow rate of the compressed air for the 2F nozzle and the voltage used to create mechanical vibrations in the US nozzle are the main factors governing the droplet size. An additional water cooling system of the cyclone (12 °C, flow rate 300 cm³.min⁻¹, tube diameter 4 mm) (Fig. 2A) was used to cool down the cyclone surface. This arrangement was designed to prevent excessive thermal degradation of the adhered powder product unless its use was prohibited by reaching the dew point of the system for given operating conditions. The specific process parameters were optimized according to the physical properties of the atomized solution, i.e., viscosity, surface tension. The feed flow rate (5 cm³.min⁻¹) was maintained by peristaltic pump Perysys, and the drying air flow rate was set to a constant value of 31.5 m³.hr⁻¹. Each batch contained 100 cm³ of feed to ensure a comparable processing time for all experiments, i.e., approximately 30 min, including the time needed for the device cool-down procedure. All spray-dried products were stored overnight in a vacuum desiccator, and the enzyme activity was analyzed the following day.

2.6. Characterization of powders

The particle size distribution (PSD) and swelling were studied using a static light scattering method in a wet mode (Horiba Partica LA-950 S2). Before PSD measurement, particles were dispersed in absolute ethanol and sonicated for 5 min to break apart temporary agglomerates. The particle suspension was then added under constant stirring into a quartz sample cell prefilled with absolute ethanol. Sample preparation for swelling experiments with

Table 1
Prepared carrier solutions and conditions of spray-drying.

code	nozzle type	operating conditions	carrier material	feed concentration w/w %	W_{TPP}^*	surface tension [mN.m ⁻¹]
A	2F	2F ^{**}	maltodextrin	3.0	–	71.43 ± 0.04
B1	US	3.5 V	chitosan	0.5	0.00	68.13 ± 0.05
B2	US	4.0 V	chitosan	0.5	0.08	67.87 ± 0.09
B3	US	5.0 V	chitosan	0.5	0.16	67.63 ± 0.05
B4	US	7.2 V	chitosan	0.5	0.32	64.97 ± 0.11
B5	2F	2F ^{**}	chitosan	1.0	0.00	74.50 ± 0.08

* W_{TPP} is defined as (weight of TPP)/(weight of chitosan)

** 0.7 mm nozzle tip, 1.4 mm nozzle cap diameter, atomizing air flow rate 473 dm³.hr⁻¹

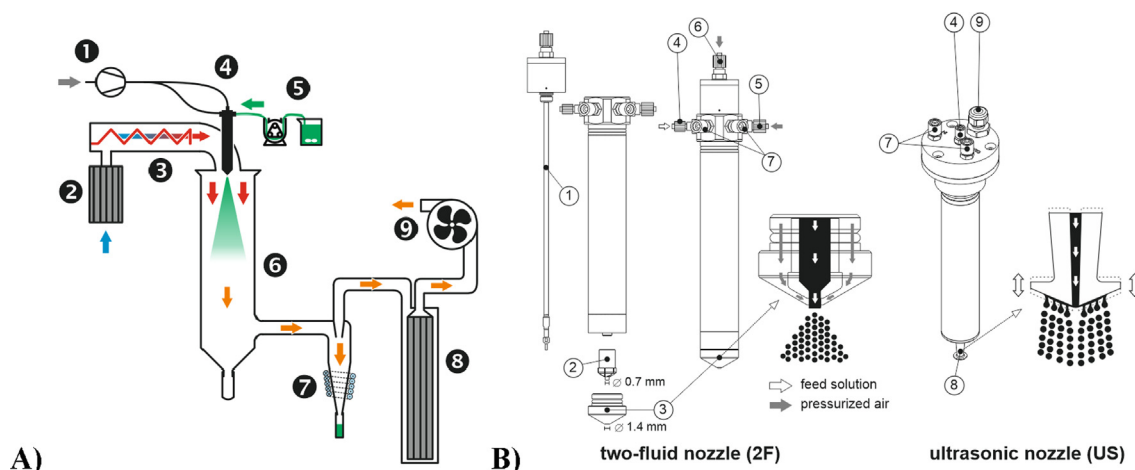


Fig. 2. A) Scheme of spray-drier Büchi B-290 with 2F nozzle; 1 - compressor, 2 - air filter, 3 - heater, 4 - nozzle, 5 - atomized solution, 6 - drying chamber, 7 - cyclone for product separation with optional cooling loop, 8 - outlet filter, 9 - aspirator; B) scheme of two-fluid nozzle (left) and ultrasonic nozzle (right); 1 - cleaning needle, 2 - nozzle tip, 3 - nozzle cap, 4 - feed inlet, 5 - inlet of atomizing gas, 6 - pressurized gas for cleaning nozzle, 7 - inlet/outlet of heating/cooling medium for the nozzle, 8 - atomizing surface, 9 - power cable.

chitosan particles was the same, except using aqueous media in the sample cell (demineralized water, Tricine-KOH buffer, $0.2 \text{ mol}\cdot\text{dm}^{-3}$, $\text{pH } 8.0 \pm 0.05$). The dynamics of swelling behavior was monitored at the beginning of the experiment and after 10 min. All measurements were performed in triplicates.

The zeta potential of hydrated particles was measured using the Zetasizer Nano-ZS (Malvern Instruments, UK). The samples were prepared as follows: *i*) spray-dried particles were dispersed in absolute ethanol and sonicated for 5 min; *ii*) the mixture was transferred into demineralized water and centrifuged; *iii*) supernatant was discarded, particles resuspended in fresh water and centrifuged (four times); *iv*) collected particles were redispersed in KCl solution ($0.01 \text{ mol}\cdot\text{dm}^{-3}$) and measured in triplicates.

Scanning transmission electron microscope (STEM) VEGA 3SBU (Tescan) was used to observe particle size and surface morphology. A powder sample was attached to a carbon conductive tape, and the surface was sputter-coated with 5 nm gold layer (Emitech K550X) to prevent sample charging and drift during image acquisition. All measurements were performed at the acceleration voltage of 19 kV.

Residual moisture content was analyzed gravimetrically by heating a known mass of sample at $200 \text{ }^\circ\text{C}$ while monitoring the weight loss. The measurement was terminated when a constant mass of the sample was reached, indicating that all free moisture was removed. All measurements were performed in triplicates.

The flowability of prepared powders was determined by the Carr's Index (also known as Compressibility Index) [35], which was selected as a suitable powder flowability indicator for a limited amount of spray-dried sample, prohibiting the application of conventional powder flow rheometers. Carr's index is defined as $\text{CI} = (\rho_{\text{tapped}} - \rho_{\text{bulk}}) / \rho_{\text{tapped}} \cdot 100\%$, where ρ_{tapped} and ρ_{bulk} are tapped and bulk density of spray-dried samples. All measurements were performed in triplicates.

2.7. Determination of protein content

The Bradford method was used for the determination of protein content. It is based on the shift of absorbance maximum of Coomassie Brilliant Blue G-250 dye (CBB) from $\lambda = 465$ to 595 nm in the presence of a protein [33]. This change is linked with the binding of amino acids, e.g., arginine, histidine, lysine, to the dye [36]. As the exact extent of the protein binding depends on the unique composition of a given protein, i.e., the total number of binding

amino acids, the choice of standard protein is very important as its amino acid composition should be as close to the analyzed protein as possible. In this case, bovine serum albumin (BSA) was used as a standard protein according to the protocol described elsewhere [31].

The CBB reagent was prepared as follows: 10 mg of Brilliant Blue G dye was dissolved in 7.1 cm^3 of absolute ethanol; 14 cm^3 of concentrated phosphoric acid was added and diluted with 121 cm^3 of demineralized water. The reagent was filtered and stored in the dark at $25 \text{ }^\circ\text{C}$ [32,33]. Protein samples were prepared as follows: *i*) 20 mg of BSA was dissolved in 10 cm^3 of demineralized water and a calibration concentration range up to $1.0 \text{ mg}\cdot\text{cm}^{-3}$ was prepared; *ii*) amount of 10 mg of lyophilized alliinase was dissolved in 1 cm^3 of demineralized water and diluted to the final concentration of $1.0 \text{ mg}\cdot\text{cm}^{-3}$.

Due to unfavorable interactions amongst alliinase, carrier materials and the CBB reagent, spray-dried samples containing BSA as a model compound (M_w 66.5 kDa) instead of alliinase (a dimer of two subunits of M_w 51.5 kDa each [37]) were used to determine the encapsulation and entrapment efficiency (similar molecular weight and amino acid composition of both proteins ensure similar behavior). The encapsulation efficiency indicates the effectivity of the spray drying process, i.e., how much protein is recovered within the powder product. Soluble samples (A, B1), containing the appropriate amount of BSA to obtain 2% w/w powder product, were used in this experiment: 20 mg of the sample was dissolved in demineralized water and used for analysis. The encapsulation efficiency was defined as the amount of protein in the spray-dried sample determined with the Bradford assay divided by the theoretical amount corresponding to 100% protein recovery. The entrapment efficiency was defined for the insoluble samples (B2 to B4) as the amount of protein tightly entrapped within the insoluble particles divided by the total amount of protein present. First, 20 mg of the sample was dispersed in 0.5 cm^3 of absolute ethanol, sonicated for 15 min, centrifugated and the supernatant was analyzed for the protein content. The samples were analyzed as follows: 20 μL was added in a Greiner 96 flat transparent well plate mixed with 180 μL of the CBB reagent. The samples were incubated at $25 \text{ }^\circ\text{C}$ for 5 min while mixing, and the absorbance at a wavelength of 595 nm was measured using spectrophotometer Tecan infinite M200 PRO. All samples were measured in triplicates at once, and the measurement cells were checked for the formation of agglomerates after each measurement.

2.8. Determination of the specific activity of encapsulated alliinase

L-lactate dehydrogenase (LDH) catalyzed reduction of the pyruvate to lactate (Fig. 3) was used for the indirect determination of alliinase activity as the alliin formation itself cannot be quantified spectrophotometrically. This coupled reaction is linked with a significant decrease in absorbance at $\lambda = 340$ nm thanks to the oxidation of NADH to NAD⁺ [38]. For accurate determination of the specific activity of alliinase, defined as micromoles of substrate transformed per second per milligram of pure protein [$\mu\text{mol}\cdot\text{s}^{-1}\cdot\text{mg}^{-1}$], it is essential to ensure that all active sites of alliinase are saturated with substrate, i.e., the reaction must follow zero-order kinetics.

Prior to the enzymatic assay, a series of experiments was performed to determine suitable initial concentrations of reagents, i.e., alliin, NADH and LDH, that ensure the zero-order kinetics. The experimental conditions were: 100 μL of the reaction mixture containing alliin (200 $\text{mmol}\cdot\text{dm}^{-3}$), NADH (0.8 $\text{mmol}\cdot\text{dm}^{-3}$), PLP (0.02 $\text{mmol}\cdot\text{dm}^{-3}$), LDH (0.25 v/v %) and alliinase (lyophilized – 12.5 $\mu\text{g}\cdot\text{cm}^{-3}$; spray-dried powder with the same or lower theoretical enzyme content) was prepared immediately before the measurement in a Greiner 96 flat transparent well plate, and the absorbance was measured by the Tecan infinite M200 PRO spectrophotometer at 340 nm.

In the case of maltodextrin-based particles, their appropriate amount was dissolved in the Tricine-KOH buffer (0.2 $\text{mol}\cdot\text{dm}^{-3}$, pH 8.00 \pm 0.05) and an aliquot was assayed immediately. Chitosan-based particles were suffering from poor wetting and formation of larger agglomerates, which was noticed even in the presence of surfactants and vigorous mixing. In this case, chitosan-based powder (10 mg) was dispersed in 200 μL of absolute ethanol (4 °C), sonicated for 10 s (132 kHz; 26.7 W), diluted with 5 cm^3 of cold Tricine-KOH buffer (4 °C) and an aliquot was checked for the enzyme activity. To minimize the negative effects of ethanol [39], all steps were performed at low temperature followed by instant mixing with the cold buffer. The influence of ultrasound on alliinase activity was neglected since it has been reported that the activity of alliinase and other enzymes was rather enhanced in the presence of mild ultrasonic irradiation [40,41]. This procedure ensured: *i*) fast and homogenous wetting of chitosan particles; *ii*) a suspension of individual particles that do not tend to agglomerate or sediment, which is essential to properly investigate the overall rate of alliin production in individual particles and to assess the effect of the spray-drying process parameters on alliinase stability.

The Michaelis–Menten kinetic constants of free and encapsulated alliinase, i.e., the maximum specific velocity (V_{max}) and Michaelis–Menten constant (K_{M}), were calculated by non-linear least-square regression of V_0 - S_0 data using SigmaPlot 11 (Systat Software Inc., Chicago, IL), where the initial reaction velocity (V_0) was determined for alliin concentration (S_0) in the range of 0.05 to 200 $\text{mmol}\cdot\text{dm}^{-3}$.

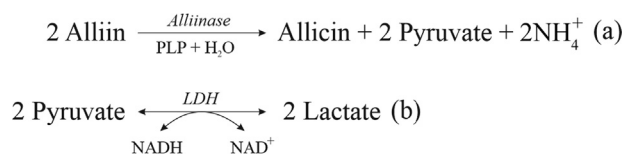


Fig. 3. (a) enzymatic formation of alliin from alliin; (b) coupled reaction of pyruvate, co-product of the reaction of alliin with alliinase, with NADH and LDH used for the UV–VIS spectroscopic assay.

2.9. Influence of heat stress

To compare the carrier materials and their ability to protect the enzyme against the thermal stress, maltodextrin and chitosan particles with encapsulated alliinase and a sample of lyophilized alliinase were exposed to elevated temperature in the oven at 100 °C for 30 min followed immediately by the LDH enzyme assay.

2.10. Antibacterial susceptibility testing

Luria-Bertani medium (LB) used for bacterial cultivation was prepared as follows: 20 g of LB salt mixture (10 g Tryptone, 5 g yeast extract, 5 g NaCl) was dissolved in 1 dm^3 of demineralized water, and pH was adjusted to 7.2–7.4 with sodium hydroxide solution (1 $\text{mol}\cdot\text{dm}^{-3}$). Bacterial colonies were resuspended in 10 cm^3 of LB medium and grown overnight at 37 °C. Bacterial suspension (0.1 cm^3 , OD₆₀₀ = 0.4) was spread onto the surface of LB agar plates (1.5 g of agar per 100 cm^3 of liquid LB medium).

The antimicrobial effects of spray-dried samples (A, B1–B4) with encapsulated alliinase (2% w/w) were tested against Gram-negative bacteria *Escherichia coli*. For this purpose, spray-dried chitosan microparticles (B1) with encapsulated alliin (2% w/w) were prepared to ensure better manipulation and homogenous distribution of the substrate within the sample. The experimental set-up illustrated in Fig. 4 can be described as follows: *i*) a mixture of powders is placed in a 3D printed holder (15.2 mm diameter, 2 mm height, 1% w/w alliin, 1% w/w alliinase in the reaction mixture, 40 mg total), covered by a permeable dialyztion membrane secured with a retaining ring (Fig. 4 a, b); *ii*) the holder, placed on a Petri dish with inoculated bacteria, is incubated at 37 °C for 24 h. The water vapor is transported through the membrane towards the sample fixed in the protrusion of the holder. Upon hydration of the sample, alliin released from chitosan carriers is enzymatically converted to alliin, transported as vapor across the membrane to bacteria (Fig. 4 c). Hydration of the sample was achieved *i*) actively - the addition of alliin solution to the sample; *ii*) passively - water uptake from humid air.

After incubation, alliin's antibacterial activity can be observed as a zone of inhibition emerging under the holder. Blank chitosan particles, i.e., without enzyme/substrate, were used as a negative control. Kanamycin, aminoglycoside bactericidal antibiotic, was used as a positive control applied on a paper disc (50 $\text{mg}\cdot\text{cm}^{-3}$, 0.02 cm^3).

3. Results and discussion

This section is presented as follows: *i*) rheological properties of feed solutions; *ii*) particle characterization (PSD, surface morphology, powder flowability, zeta potential, residual moisture content); *iii*) the specific activity of alliinase encapsulated in maltodextrin and chitosan carriers as a function of the inlet temperature of drying air; *iv*) swelling behavior, and its effect on the observed enzyme activity of immobilized alliinase; *v*) antibacterial susceptibility testing.

3.1. Rheological properties of feed solutions

The physicochemical characteristics of the feed solution, i.e., viscosity, density, and surface tension govern along with the type of atomizer formation of the spray. In general, their higher values contribute to a larger mean size of the final powder product [42]. The experimentally measured values of surface tension of atomized feed solutions are summarized in Table 1. The surface tension value of 3.0% maltodextrin (A) was comparable to pure water ($\sigma_{\text{water}} = 72.53 \text{ mN}\cdot\text{m}^{-1}$ at 20 °C). The surface tension of

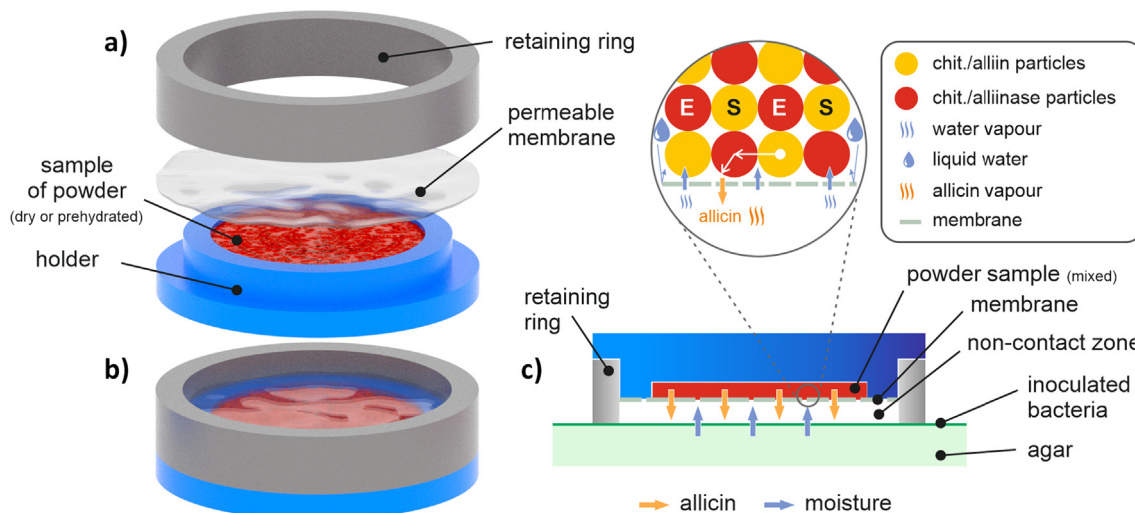


Fig. 4. The experimental set-up of non-contact diffusion method; a) exploded diagram of customized 3D printed holder; b) assembled holder preventing physical contact of powder and bacteria; c) holder placed on the inoculated agar plate.

0.5% chitosan solution remained constant up to $W_{TPP} = 0.16$ (sample B3) with a noticeable drop at $W_{TPP} = 0.32$.

The results of rheological measurements performed at 23 °C are presented in Fig. 5. Maltodextrin solution displayed typical Newtonian liquid behavior with a constant dynamic viscosity of 1 mPa.s across an investigated range of shear rates. The chitosan carriers displayed distinct behavior depending on chitosan concentration and TPP/chitosan ratio (W_{TPP}). Samples with no TPP (B1 and B5) and low TPP content (B2, B3) showed Newtonian liquid behavior as well, whereas solutions with the highest TPP amount (B4) exhibited non-Newtonian pseudoplastic characteristics, i.e., dynamic viscosity decreased with shear rate. The increase of chitosan concentration leads to a higher value of dynamic viscosity. However, the addition of low amounts of TPP (B2, B3) decreased the dynamic viscosity in comparison to the non-cross-linked sample of the same chitosan concentration.

3.2. Characterization of spray-dried particles

The comparison of maltodextrin (A) and chitosan (B1-5) microparticles prepared by Büchi B-290 and their respective values of volume mean diameter $D[4,3]$ and span are summarized in Table 2. Span, the indicator of the distribution width, is defined as $(d_{90} - d_{10})/d_{50}$, where d_{90} , d_{10} and d_{50} are the upper decile, lower

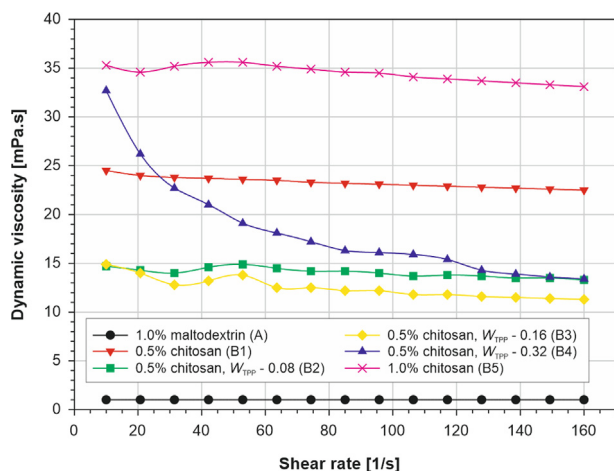


Fig. 5. Dynamic viscosity as a function of shear rate for atomized solutions.

decile, and median. In all cases, the calculated span number was very close to one, i.e., the size distribution can be considered narrow [43,44]. The PSDs of analyzed samples showing log-normal distribution are illustrated in Fig. 6A (samples A and B5, 2F nozzle) and Fig. 6B (samples B1 and B4, US nozzle).

The volume mean diameter $D[4,3]$ of maltodextrin particles was larger than chitosan particles prepared by the same 2F nozzle (Fig. 6A), which can be explained by different rheological properties of atomized solutions and higher content of soluble solids. The choice of the inlet temperature (T_{in} varied in the range 110 °C to 180 °C) had no particular effect on the PSD of both chitosan and maltodextrin microparticles. With the increasing amount of TPP cross-linker (B1 to B4) in chitosan-based particles, the increasing value of mean particle size was observed (Fig. 6B), shifting the PSD to the right. This observation is in agreement with previous studies [45,46] conducted using 2F atomizers but with generally larger particles due to the use of ultrasonic nozzle.

The zeta potential values (ζ) are summarized in Table 2 (note: samples A, B1 and B5 are soluble in KCl solution). The observed zeta potentials of samples B2 ($W_{TPP} = 0.08$) to B4 ($W_{TPP} = 0.32$) were not significantly different, which is in agreement with the previous studies concerning the stability of spray-dried chitosan particles prepared by 2F nozzle [45].

The Carr's index values (Table 2) indicate the flowability of spray-dried particles. Given by small particle size, calculated CI values are relatively high ($CI \geq 35$), indicating cohesive powders with poor flowability. However, the flow properties can be eventually enhanced with suitable additives, e.g., magnesium stearate. Moreover, the results suggest that TPP addition positively impacts powder flowability as the CI decreases with higher W_{TPP} .

The typical morphologies characteristic for each formulation can be observed in Fig. 7. Chitosan particles without cross-linker (B1 and B5) feature spherical shape and brain-like surface structure, whereas maltodextrin particles have a smooth surface but visibly irregular shape caused by buckling of the particles after cooling. Cross-linked chitosan particles have a smoother surface and deflated shape resembling maltodextrin carriers which is more accentuated with increasing W_{TPP} ratio (B2 to B4).

3.3. Residual moisture analysis

Chitosan and maltodextrin particles prepared at three different inlet temperatures of the drying air (110 °C, 130 °C and 180 °C)

Table 2
Summary of the particle size distribution measurements, zeta potential (ζ) and Carr's index (CI).

code	T_{in} [°C]	T_{out} [°C]	$D[4,3]$ [μm]	d_{50} [μm]	d_{10} [μm]	d_{90} [μm]	span	ζ [mV]	CI*
A	110	53	7.5 ± 2.5	7.2	4.6	10.9	0.9	–	44 ± 3
A	180	86	8.1 ± 2.9	7.7	4.8	12.0	0.9	–	
B1	120	54	6.5 ± 2.4	6.2	3.9	9.8	1.0	–	54 ± 1
B2	120	54	6.2 ± 2.1	6.3	4.0	9.9	1.0	22.0 ± 1.8	45 ± 2
B3	120	54	7.5 ± 2.5	7.2	4.7	10.9	0.9	22.0 ± 2.4	39 ± 1
B4	120	57	9.3 ± 3.1	8.9	5.6	13.6	0.9	23.1 ± 1.0	36 ± 1
B5	110	56	4.2 ± 1.8	3.9	2.3	6.5	1.1	–	51 ± 2
B5	180	89	3.3 ± 1.4	3.0	2.0	6.6	1.1	–	

* Measured for the samples prepared at $T_{in} = 120$ °C

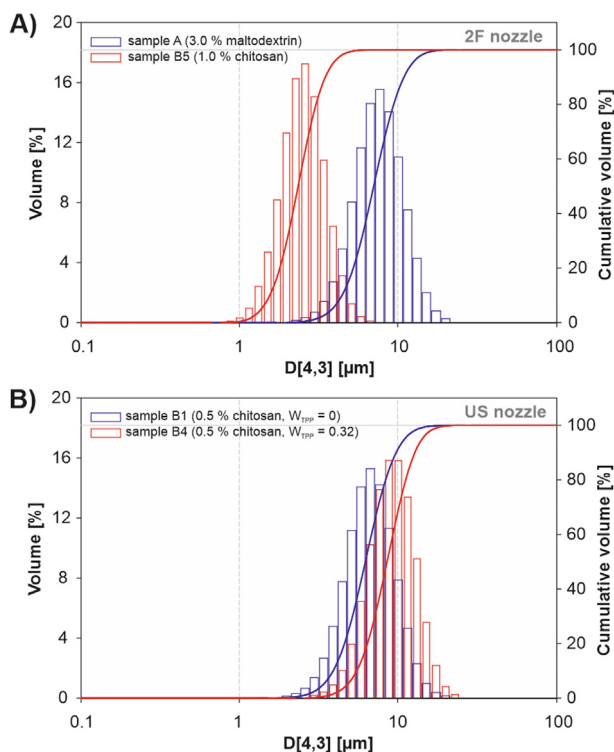


Fig. 6. Particle size distributions: A) maltodextrin (sample A) and chitosan (B5) particles prepared by 2F nozzle at 110 °C; B) non-cross-linked (B1) and cross-linked (B4) chitosan particles prepared by US nozzle at $T_{in} = 120$ °C.

were analyzed (Table 3). No major change in residual moisture of chitosan or maltodextrin was observed for higher temperatures of the drying air. However, significant differences were observed comparing maltodextrin and chitosan particles, which is in agreement with the theory of convective drying [47]. The formation of solid crust around a liquid core ends the first period of drying that is not limited by the moisture transport to the surface. The crust is formed once the local concentration of solute material exceeds its solubility in the used solvent. Compared to chitosan, the higher water solubility of maltodextrin results in latter crust formation and longer duration of the first drying period characterized by the maximum drying rate. This is reflected in $\sim 35\%$ lower residual moisture content in maltodextrin particles and lower temperatures of the outlet stream leaving the drying chamber.

3.4. Effect of temperature on specific enzyme activity

The variation of the inlet temperature of the drying air T_{in} (110 °C to 180 °C) allows to *i*) isolate the effect of heat stress on the specific activity of encapsulated alliinase; *ii*) compare the protective ability of maltodextrin and chitosan as carrier material;

iii) optimize the spray-drying conditions in respect to the alliinase activity. All results are presented as the relative activity, i.e., the ratio of the specific activity of encapsulated and lyophilized alliinase. No catalytic activity was observed for a negative control (alliinase-free chitosan and maltodextrin particles), which indicates that the material of carriers does not interfere with the colorimetric LDH assay.

Experimentally determined values of specific activities for maltodextrin and chitosan-based particles are not directly comparable due to different sample preparation for the enzymatic assay, i.e., the use of ethanol and ultrasonic bath for dispersion of chitosan particles. Following the same protocol, the maltodextrin particles lost approximately 40% of the specific activity compared to the dry sample dissolved directly in the buffer solution. For a better representation of thermal effects on enzyme activity of both polymers, the results summarized in Table 4 were normalized according to the highest specific activity of samples of the corresponding polymer spray-dried at 110 °C (the last column in Table 4 and Fig. 8).

Following this approach, we can compare the protective ability of maltodextrin and chitosan without further uncertainty caused by the differences in sample preparation for the UV–VIS assay. In agreement with the theory of enzyme degradation [39], the decrease of alliinase activity at higher temperatures was observed for both carrier materials. Based on the results, the optimal operating inlet temperature was 120 °C for both polymers with the use of external cooling for chitosan particles. The lower temperatures, i.e., 110 °C, resulted in excessive deposition of materials on the drying chamber walls and the cyclone and a lower yield. The temperature of inlet air above 130 °C did not significantly improve product quality in terms of the yield or residual moisture content.

The activity of alliinase encapsulated in maltodextrin was unaffected by the drying temperature up to 160 °C. Surprisingly, alliinase remained highly active even at 180 °C (outlet temperature exceeding 86 °C), losing only 21% of the activity compared to maltodextrin spray-dried at 110 °C. Alliinase encapsulated in chitosan showed a gradual decrease with increasing inlet temperature resulting in 70% lower activity for $T_{in} = 180$ °C compared to alliinase encapsulated at 110 °C. The results indicate that maltodextrin is significantly more effective in protecting the encapsulated alliinase against thermal stress compared to chitosan. This phenomenon is attributed to better protective properties of maltodextrin thanks to a higher amount of hydroxyl groups. Maltodextrin carrier mimics the hydrogen bonding between protein and water molecules in a cellular environment. In this way, the native conformation of the protein is maintained even in a solid state [48]. Moreover, the negative effect of moisture, which is 4–times higher in chitosan compared to the maltodextrin particles, on protein stability is well documented [30,49]. Thereby, the protective effect of maltodextrin can be further magnified, lowering the moisture content in the final product.

The protective properties of chitosan and maltodextrin against the thermal stress were compared to purified lyophilized alliinase.

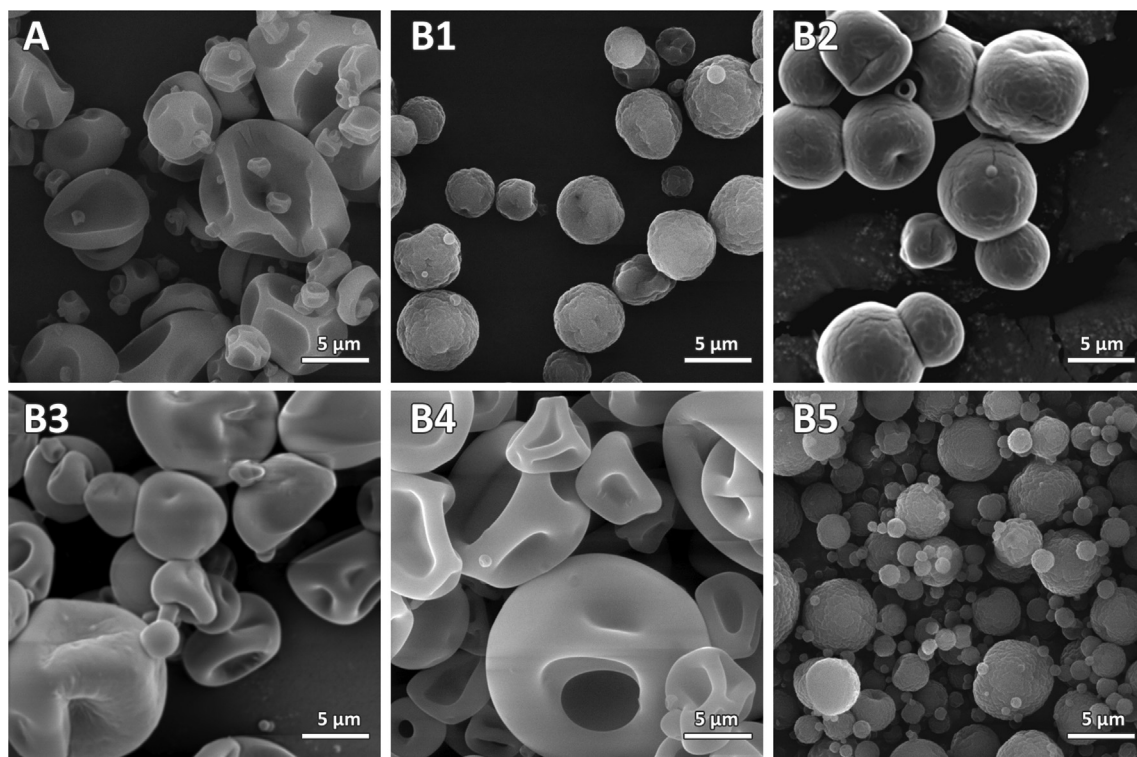


Fig. 7. Characteristic surface morphologies (SEM) of maltodextrin (A) and non-cross-linked (B1, B5) and cross-linked chitosan microparticles (B2 - $W_{TPP} = 0.08$, B3 - $W_{TPP} = 0.16$, B4 - $W_{TPP} = 0.32$).

Table 3

Residual moisture content analysis for maltodextrin and chitosan particles prepared at different inlet temperatures of the drying air.

code	carrier	inlet temperature [°C]	outlet temperature [°C]	residual moisture content [%]
A	maltodextrin	110*	53	12.7 ± 0.1
A	maltodextrin	130	63	13.6 ± 0.9
A	maltodextrin	180	86	9.1 ± 2.2
B5	chitosan	110*	56	44.5 ± 4.2
B5	chitosan	130	65	46.1 ± 2.8
B5	chitosan	180	89	51.6 ± 2.5

* external cooling is not applicable due to moisture condensation

Table 4

Summary of the specific activity of alliinase encapsulated in maltodextrin and chitosan carriers prepared at various temperatures of the drying air.

code	T_{in} [°C]	T_{out} [°C]	cooling	specific activity [$\mu\text{mol}\cdot\text{s}^{-1}\cdot\text{mg}^{-1}$]*	relative activity [%]**	normalization [%]
A	110	53	No***	1.40 ± 0.04	98.4 ± 2.8	100.0 ± 2.9
A	120	56	No***	1.27 ± 0.01	89.2 ± 0.3	90.7 ± 0.7
A	130	63	Yes	1.30 ± 0.07	91.3 ± 4.9	92.9 ± 5.0
A	160	79	Yes	1.31 ± 0.06	92.0 ± 4.4	93.6 ± 4.3
A	180	86	Yes	1.10 ± 0.05	77.7 ± 3.6	78.6 ± 3.6
B5	110	56	No***	0.71 ± 0.06	45.4 ± 3.7	100.0 ± 8.5
B5	120	59	Yes	0.62 ± 0.02	40.0 ± 1.5	87.3 ± 2.8
B5	130	65	Yes	0.47 ± 0.03	32.4 ± 1.8	66.2 ± 4.2
B5	160	80	Yes	0.29 ± 0.03	18.4 ± 1.8	40.8 ± 4.2
B5	180	89	Yes	0.21 ± 0.01	13.7 ± 0.4	29.6 ± 1.4

* specific activity is defined as micromoles of substrate per second per mg of pure protein; protein content was determined by the Bradford assay

** the specific activity of lyophilized alliinase represents 100%, i.e., $1.43 \pm 0.02 \mu\text{mol}\cdot\text{s}^{-1}\cdot\text{mg}^{-1}$ and $1.55 \pm 0.05 \mu\text{mol}\cdot\text{s}^{-1}\cdot\text{mg}^{-1}$ for maltodextrin (A) and chitosan (B5) particles, respectively

*** external cooling is not applicable due to moisture condensation

Visible degradation of pure lyophilized alliinase was observed after the heating experiment (100 °C, duration of 30 min) due to the color change and a partial loss of solubility. Moreover, no catalytic activity was observed during the LDH assay. Alliinase encapsulated into maltodextrin and chitosan carriers lost only 20% and 26% of

the initial activity of the spray-dried product, respectively. The total degradation of the encapsulated enzyme (samples A, B5) was achieved at 200 °C when no catalytic activity was observed, but the physical appearance and solubility of particles in pure water remained unaffected.

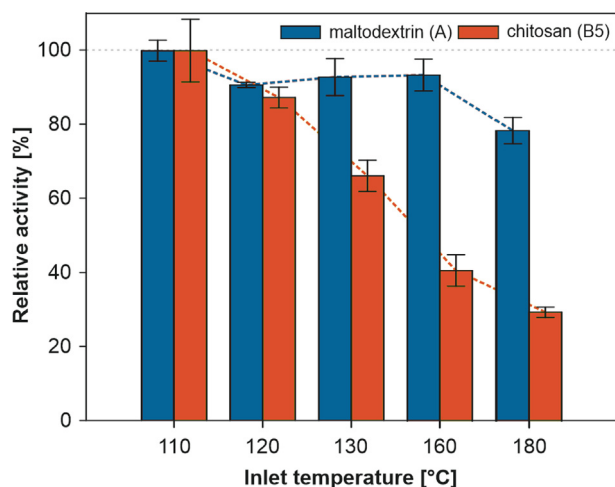


Fig. 8. The enzyme activity of maltodextrin and chitosan particles vs. inlet drying temperature.

3.5. The effect of cross-linking on alliin production

Chitosan particles incubated in neutral or slightly basic aqueous media, i.e., the Tricine-KOH buffer and demineralized water, swell by incorporating water molecules and form a porous heterogeneous structure through which molecules can be transported [50,51]. Their swelling behavior can be greatly modified by cross-linking with tripolyphosphate anions (TPP). The extent of particle swelling can be described by the swelling ratio X_{swell} , defined as the ratio of the mean particle size in aqueous media and a dry state. The particles with a varying W_{TPP} produced by ultrasonic nozzle were used for the investigation of swelling behavior. The upper limit of the cross-linking ratio was set as $W_{\text{TPP}} = 0.32$ for the following reasons: *i*) rheological properties of polymeric solutions with W_{TPP} greater than 0.32 were not compatible with the atomization via ultrasonic nozzle; *ii*) produced particles were prone to the formation of agglomerates, due to the high TPP anion surface concentration balancing out the positive charge of protonated chitosan chains [52]. Demineralized water was used as an aqueous reference medium allowing comparison with previous studies, while the Tricine-KOH buffer provided information about particle behavior in the environment used for the UV-VIS LDH assays. The obtained results are summarized in Table 5.

Depending on the cross-linking ratio and type of solvent, we observed two different types of particle behavior, i.e., particle dissolution and swelling. In both media, the swelling was suppressed at higher cross-linking ratios. This trend is in agreement with previously published experimental results [45]. The higher cross-linker concentration leads to tighter bonds between individual chitosan chains, which prevents more extensive swelling. Moreover, we observed significant differences in particle behavior in Tricine-KOH buffer ($0.2 \text{ mol}\cdot\text{dm}^{-3}$, pH 8.00 ± 0.05) and demineral-

ized water. The swelling ratios of cross-linked particles in demineralized water were significantly higher. Pure chitosan particles (sample B1) were dissolved in water immediately. No significant change after 10 min of incubation was observed in either media, i.e., particles increased their volume instantly, and their mean size did not change significantly (Table 5).

The observed differences in the swelling behavior in aqueous media have an important impact on the effective diffusion coefficients of compounds transported within the structure. The effective diffusion coefficient is derived from the coefficient describing free diffusion in a corresponding homogenous liquid environment considering various porous structure properties: porosity, tortuosity and hindrance factor. The increasing value of the swelling ratio translates into the higher porosity and lower tortuosity of the chitosan matrix, which results in a higher diffusion coefficient of transported solutes. Moreover, based on the theory of enzyme kinetics [39], the kinetic parameters, i.e., Michaelis constant, maximum reaction rate V_{max} , are lowered upon enzyme immobilization leading to a lowered rate of reaction regardless of the substrate diffusion limitations. However, these differences in kinetic parameters cannot be observed separately, as they are always connected with substrate diffusion limitations. The connection between the structure of the carrier polymer and the rate of alliin production is discussed in the following text.

Under the conditions described in the methods section, the process of alliin transformation can be described as follows: *i*) particles with encapsulated alliinase are dispersed/dissolved in the solution; *ii*) alliin, LDH and NADH are added; *iii*) alliin is either directly transformed in the solution or transported through the porous structure of swelled particle to the active site of immobilized alliinase, transformed to alliin which is then, along with the side products, transported to the bulk solution; *iv*) side product pyruvate is reduced to lactate while NADH is oxidized and a decrease in absorbance at $\lambda = 340 \text{ nm}$ is monitored.

The LDH assay results for all prepared samples with encapsulated alliinase (2% w/w) are in Fig. 9. The absorbance decrease over time is attributed to the combination of both the reaction occurring in the bulk liquid (free enzyme) and inside/on the surface of swelled carriers (immobilized enzyme). The specific enzyme activity for every sample calculated from the initial slope of the absorbance vs. time curve (0 to 100 s) was compared with the specific activity of pure alliinase (Table 6).

The alliinase encapsulated in soluble maltodextrin particles (sample A) was upon homogenization instantly liberated to the reaction mixture, which resulted in very fast, unhindered alliin conversion to alliin. In this scenario, the substrate transport to the active site of the enzyme is not affected by the carrier's material properties. Observed enzyme activity for swellable chitosan carriers without TPP (samples B1 and B5) was, compared to sample A, significantly reduced since the chitosan matrix acts as a barrier hindering the mass transport of reactants and products. However, even though samples B1 and B5 share the same material properties, the calculated relative specific activity of sample B5 was 27%

Table 5
Results of swelling behavior experiments for samples B1-B4.

code	W_{TPP}	demineralized water				buffer			
		0 min		10 min		0 min		10 min	
		mean size [μm]	X_{swell}^*	mean size [μm]	X_{swell}	mean size [μm]	X_{swell}	mean size [μm]	X_{swell}
B1	0.00	dissolution of particles				18.1 \pm 7.7	2.7	15.7 \pm 5.6	2.4
B2	0.08	37.6 \pm 11.4	6.1	40.6 \pm 15.1	6.5	14.4 \pm 5.7	2.3	13.8 \pm 5.2	2.2
B3	0.16	25.9 \pm 9.9	3.5	25.3 \pm 12.9	3.4	25.9 \pm 9.9	2.8	25.3 \pm 12.9	2.7
B4	0.32	11.3 \pm 3.6	1.2	10.9 \pm 3.5	1.2	11.3 \pm 3.6	1.2	10.9 \pm 3.9	1.2

* X_{swell} is defined as the mean size of the particles in aqueous media vs. mean size in a dry state

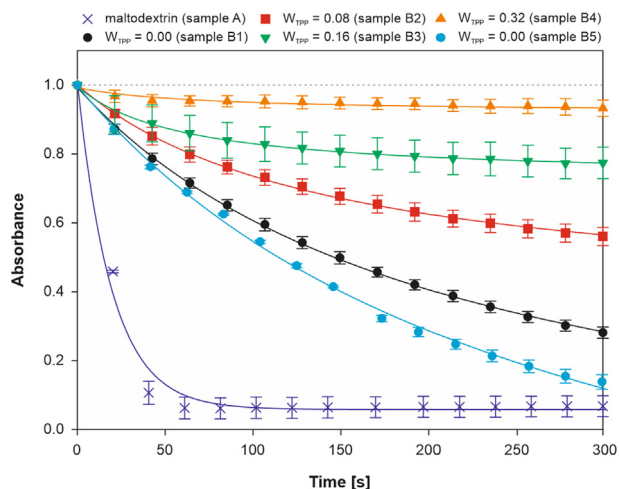


Fig. 9. UV-VIS LDH assay - the influence of carrier composition on overall enzyme production of alliin.

higher than B1. The difference can be explained by various PSD of both samples prepared by different nozzles. The mean diameter of the sample B5 prepared by 2F nozzle was almost 2-times smaller compared to B1 (Fig. 6), which results in a higher specific surface area exposed to the reaction mixture. With the addition of TPP, a significant decrease in enzyme activity was observed. With higher TPP content, chitosan chains are more densely cross-linked, which results in tighter confinement of alliinase, reduced swelling upon hydration (Table 5) and a more compact matrix hindering the mass transport considerably. Increasing of W_{TPP} from 0 to 0.08, 0.16 and 0.32 reduced the overall enzyme activity by 40%, 62% and 77%, respectively.

The typical curves of Michaelis-Menten kinetics for samples A, B5 and their corresponding standard (lyophilized alliinase) are shown in Fig. 10. The $V_{max}/V_{max,ref}$ ratio summarized in Table 6 shows that for insoluble carriers the apparent V_{max} values are with increasing W_{TPP} reduced five to more than ten times compared to standard. This result can be expected due to transport limitation hindering the substrate diffusion to the catalytic site of immobilized alliinase.

3.6. Encapsulation and entrapment efficiency

The encapsulation and entrapment efficiency were determined for water-soluble (A, B1) and swellable (B2 to B4) samples, respectively. The results are summarized in Fig. 11. Encapsulation efficiency for both pure maltodextrin and chitosan exceeds 94%. The protein losses could be attributed to adhesion to the glassware, tubing, or nozzle interface. The entrapment efficiency determined

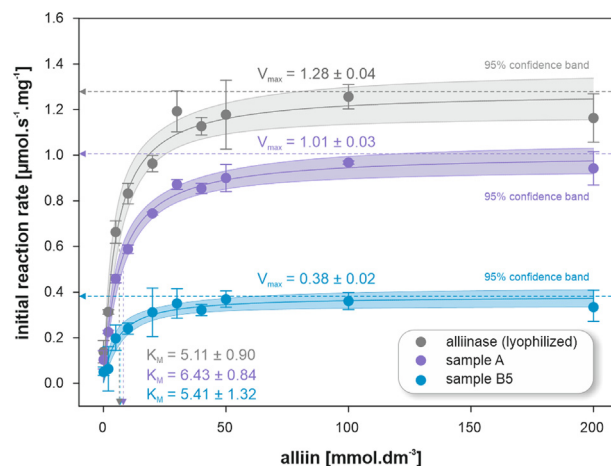


Fig. 10. Evaluation of the Michaelis-Menten kinetic constants (V_{max} and K_M) of free and encapsulated alliinase (samples A and B5).

for the insoluble samples demonstrates the ability of the carriers to immobilize the protein upon hydration in an aqueous environment. The results suggest that cross-linked chitosan carriers can hold more than 93% of initially encapsulated protein regardless of TPP amount.

3.7. Testing of antibacterial susceptibility of binary systems

The antibacterial activity of prepared samples with immobilized alliinase was tested against Gram-negative bacteria *E. coli* using two ways of alliin addition: i) a mixture of spray-dried powders with encapsulated alliin and alliinase in the dry form; ii) a sample containing encapsulated alliinase prewetted with alliin solution. In both cases, the studied sample was confined in a customized holder separated from the surroundings by a membrane permeable for water vapor and alliin (Fig. 4). The visible “coffee ring” on agar plates represents the footprint of the 3D printed holder. The positive antibacterial effect was observed as an inhibition zone emerging under the holder. As a positive control, antibiotic kanamycin was applied on a filter paper disk (20 μ L, 50 $\text{mg}\cdot\text{cm}^{-3}$).

In the first set of experiments, the dried forms of encapsulated alliinase and alliin were tested, and an antibacterial effect was visible when both types of particles were present simultaneously (Fig. 12B, “A_E + B1_S”). In this case, the enzyme was encapsulated in 20 mg of maltodextrin particles (A_E, 2% w/w), and the substrate was encapsulated in 20 mg of chitosan particles (B1_S, 2% w/w). Negative controls, alliinase encapsulated in maltodextrin particles (A_E), alliin encapsulated in chitosan particles (B1_S), pure chitosan (B1 - blank), and maltodextrin (A - blank) particles, did not

Table 6
Specific activities for all samples ($T_{in} = 120^\circ\text{C}$).

code	W_{TPP}	T_{out} [$^\circ\text{C}$]	overall specific activity [$\mu\text{mol}\cdot\text{s}^{-1}\cdot\text{mg}^{-1}$]*	relative specific activity [%]**	$V_{max}/V_{max,ref}$ [%]***
A	–	56	1.27 ± 0.01	88.8 ± 0.7	78.9
B1	0.00	54	0.23 ± 0.01	37.7 ± 1.6	20.4
B2	0.08	54	0.14 ± 0.01	23.0 ± 1.6	16.3
B3	0.16	54	0.09 ± 0.01	14.8 ± 1.6	12.2
B4	0.32	54	0.05 ± 0.02	8.2 ± 3.3	8.2
B5	0.00	59	0.62 ± 0.02	40.0 ± 1.3	29.7

* specific activity is defined as micromoles of substrate per second per mg of alliinase present in the sample

** the specific activity of lyophilized alliinase represents 100%, i.e., $1.43 \pm 0.02 \mu\text{mol}\cdot\text{s}^{-1}\cdot\text{mg}^{-1}$, $0.61 \pm 0.06 \mu\text{mol}\cdot\text{s}^{-1}\cdot\text{mg}^{-1}$ and $1.55 \pm 0.05 \mu\text{mol}\cdot\text{s}^{-1}\cdot\text{mg}^{-1}$ for samples A, B1-B4 and B5, respectively

*** V_{max} and $V_{max,ref}$ are maximal specific velocity for encapsulated and lyophilized alliinase

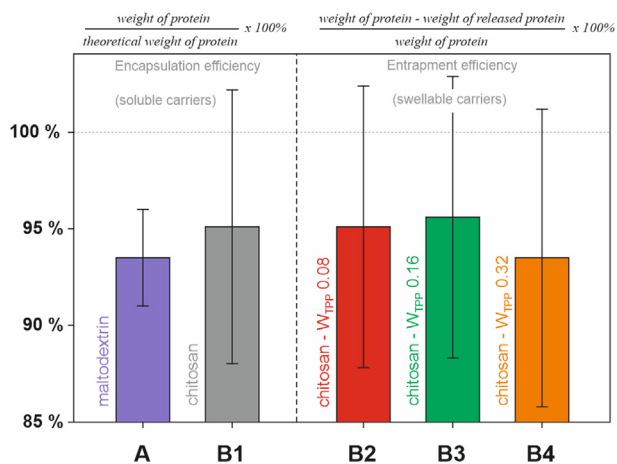


Fig. 11. The encapsulation and entrapment efficiency of spray-dried maltodextrin and chitosan carriers (A, B1) and cross-linked chitosan carriers (B2 to B4).

show any antibacterial effect (the minimum inhibitory concentration (MIC) for pure chitosan has been found between 0.38 and 0.75 mg.cm⁻³).

The effect of W_{TPP} on the antibacterial activity of B1_S (20 mg) in the mixture with chitosan carriers B1 to B4 (20 mg) is shown in Fig. 12C. The observed antibacterial performance agrees with the results of particle swelling and enzyme activity described in Section 3.5. The higher W_{TPP} (increasing from B1 to B4) resulted in a weaker antibacterial effect related to a slower alliin formation. In Fig. 12D, the influence of B1_E amount (10 to 25 mg) on the antibacterial activity in the mixture with B1_S (25 mg) is presented. Even the lowest alliinase amount (10 mg of B1_E powder, 0.2 mg of enzyme) was effective against *E. coli*.

In the second set of antibacterial tests, the spray-dried particles with encapsulated alliinase placed in the holder were pre-wetted with alliin solution (50 μ L of 100 mmol.dm⁻³) and sealed by the permeable membrane. In this case, all samples showed antibacterial activity in contrast to Fig. 12C. In some instances, the outlines of inhibition zones were larger than the footprint of the sample holder (Fig. 13). The sample A_E showed a strong bactericidal effect because of the complete dissolution of maltodextrin carriers upon alliin addition, followed by immediate alliin production (Fig. 13A). In the case of cross-linked chitosan-TPP particles, the pre-wetting enhanced the antibacterial effect, and even the sample with the highest W_{TPP} (B4_E) was effective as opposed to the dried particles solely relying on the absorption of air moisture initiating alliin dissolution, release and enzymatic conversion to alliin (Fig. 12C).

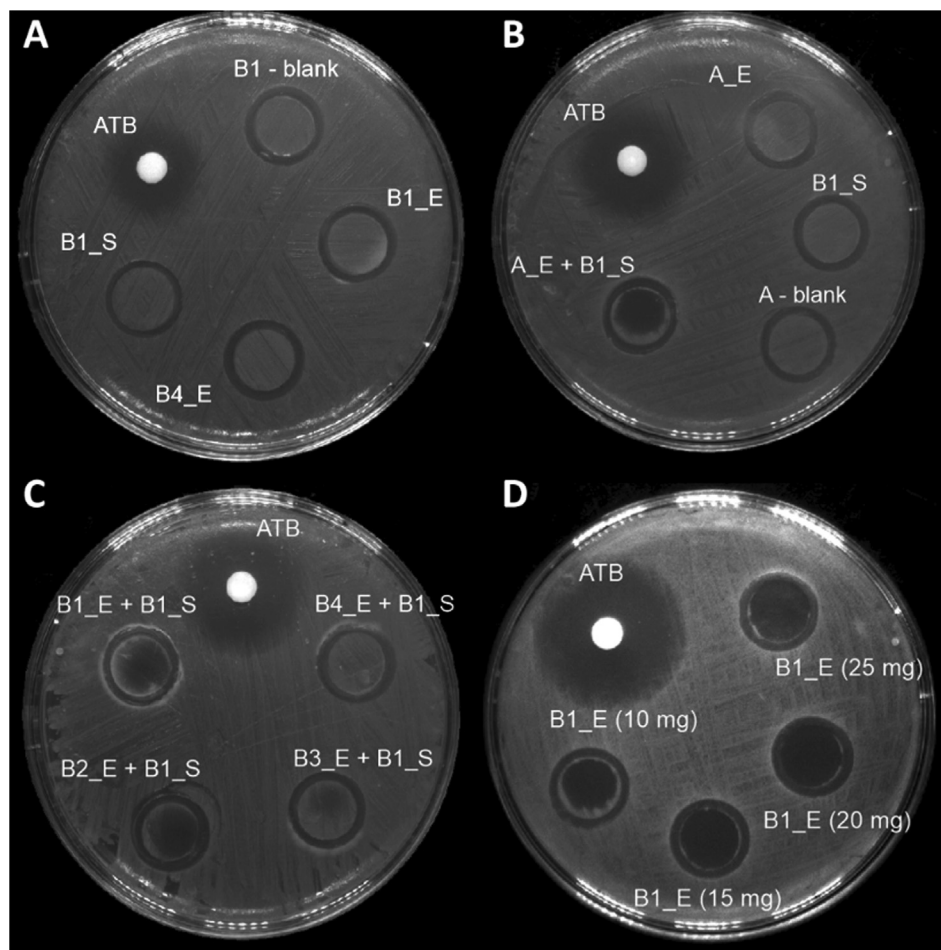


Fig. 12. Non-contact testing of antibacterial activity of binary alliin-alliinase system in powder forms (labeling – “sample formulation” – “type of encapsulated material”, i.e., “E” = enzyme, “S” = substrate and “blank” = none): A) negative controls of various chitosan particle samples (20 mg per holder); B) mixture of sample A (maltodextrin) with the encapsulated enzyme (A_E, 20 mg) and sample B1 with encapsulated alliin (B1_S, 20 mg) and corresponding negative controls (A_E, B1_S and A – blank); C) effect of increasing TPP amount in samples B1 to B4 (20 mg per holder) in the mixture with B1_S (20 mg); D) effect of the increasing amount of encapsulated enzyme in sample B1_E (10 mg to 25 mg) in the mixture with B1_S (25 mg); a positive control of kanamycin antibiotic “ATB” was used in all cases.

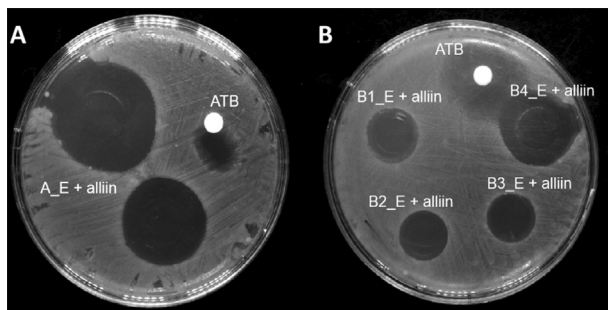


Fig. 13. Non-contact testing of antibacterial activity of binary alliin-alliinase system with encapsulated alliinase and alliin solution (50 μL of 100 $\text{mmol}\cdot\text{dm}^{-3}$): A) maltodextrin carriers (sample A) with the enzyme; B) chitosan carriers (samples B1 to B4) with the enzyme. Note: the amount of dry sample was 20 mg for all experiments; a positive control of kanamycin antibiotic “ATB” was used in all cases.

4. Conclusion

In this work, we present spray-drying as a suitable technique for encapsulation of garlic alliinase into soluble (maltodextrin, chitosan) and swellable (chitosan-TPP) micro-carriers. We studied and optimized the process parameters, e.g., the inlet temperature of the drying air, additional cooling, and type of the atomizing nozzle, to maintain a high specific activity of encapsulated alliinase in the final product. Compared to chitosan, maltodextrin showed superior properties in terms of protection of encapsulated alliinase against thermal stress, preserving more than 90% of the initial enzyme activity in the spray-dried product. In contrast to soluble maltodextrin, chitosan in combination with TPP cross-linker allows enzyme encapsulation in swellable carriers with tunable transport properties. Altering the degree of chitosan cross-linking, we can control the progress of the enzymatic reaction and tailor the production of alliin according to specific demands. The excellent protective properties of maltodextrin suggest its possible application as an excipient in chitosan particles providing an additional layer of enzyme protection during spray-drying and long-term storage. Using the innovative non-contact diffusion method, we demonstrated that the spray-dried powders activated by air moisture or the pre-wetted powder could be applied for *in-situ* generation of the therapeutically effective doses of alliin.

The knowledge about the relationship between carrier material and enzyme activity allows to prolong alliin *in-situ* formation and avoid its high local concentrations or burst release, leading to undesired side effects such as skin irritation or severe chemical burns. These findings may contribute to the development of sustainable nature-inspired products based on the controlled *in-situ* synthesis of highly reactive antibiotics from their stable precursors.

Declaration of Competing Interest

The authors declare that they have no known competing financial interests or personal relationships that could have appeared to influence the work reported in this paper.

Acknowledgment

This work was financially supported by the Technology Agency of the Czech Republic (TJ01000313), the Czech Science Foundation (GACR 17-11851Y), the OP RDE registration no.: CZ.02.2.69/0.0/0.0/19_073/0016928, funded by the ESF, grant support from Ministry of Industry and Trade (MPO 731745/2020) and the grant of Specific university research – grant No A1_FCHI_2020_004.

References

- [1] L.L. Silver, Challenges of antibacterial discovery, *Clin Microbiol Rev* 24 (1) (2011) 71–109.
- [2] J.W. Bennett, K.-T. Chung, Alexander Fleming and the discovery of penicillin, *Advances in Applied Microbiology* 49 (2001) 163–184.
- [3] A.J. Alanis, Resistance to antibiotics: are we in the post-antibiotic era?, *Archives of medical research* 36 (6) (2005) 697–705.
- [4] World Economic Forum - Global Risks Report, 12th edition, http://www3.weforum.org/docs/GRR17_Report_web.pdf.
- [5] Antimicrobial resistance: global report on surveillance 2014. http://apps.who.int/iris/bitstream/10665/112642/1/9789241564748_eng.pdf?ua=1.
- [6] Stokes, J.M., et al., A Deep Learning Approach to Antibiotic Discovery. *Cell*, 2020. 180(4): p. 688-702 e13g.
- [7] K. Gupta, R. Viswanathan, Combined Action of Streptomycin and Chloramphenicol with Plant Antibiotics against Tubercle Bacilli. Part I: Streptomycin and Chloramphenicol with Cepharanthine. Part II: Streptomycin and Alliin, *Antibiotics & Chemotherapy* 5 (1) (1955) 24–27.
- [8] Block, E., *Garlic Other Alliums*. 2010: RSC publishing Cambridge.
- [9] J.E. Lancaster, Production of flavour precursors [S-alk (en) γ -L-cysteine sulphoxides] in photomixotrophic callus of garlic, *Phytochemistry* 27 (7) (1988) 2123–2124.
- [10] I. Dini, G.C. Tenore, A. Dini, S-alkenyl cysteine sulfoxide and its antioxidant properties from *Allium cepa* var. *tropeana* (red onion) seeds, *J Nat Prod* 71 (12) (2008) 2036–2037.
- [11] R. Leontiev et al., A Comparison of the Antibacterial and Antifungal Activities of Thiosulfinate Analogues of Alliin, *Sci Rep* 8 (1) (2018) 6763.
- [12] E. Appel et al., Therapy of murine pulmonary aspergillosis with antibody-alliinase conjugates and alliin, *Antimicrobial Agents Chemotherapy* 54 (2) (2010) 898–906.
- [13] L.D. Lawson, S.M. Hunsaker, Alliin Bioavailability and Bioequivalence from Garlic Supplements and Garlic Foods, *Nutrients* 10 (7) (2018) 812.
- [14] T. Miron et al., A method for continuous production of alliin using immobilized alliinase, *Analytical Biochemistry* 351 (1) (2006) 152–154.
- [15] P. Milka, I. Krest, M. Keusgen, Immobilization of alliinase on porous aluminum oxide, *Biotechnology and bioengineering* 69 (3) (2000) 344–348.
- [16] E. Anifantaki, E. Touloupakis, D.F. Ghanotakis, Alliinase Immobilization in Calcium Alginate Beads and Layered Double Hydroxides Matrices, *Journal of Food Biochemistry* 36 (1) (2012) 12–20.
- [17] J. Ko et al., Preparation of encapsulated alliinase in alginate microparticles, *Biotechnology letters* 34 (3) (2012) 515–518.
- [18] J.Q. Zhou, J.W. Wang, Immobilization of alliinase with a water soluble-insoluble reversible N-succinyl-chitosan for alliin production, *Enzyme and Microbial Technology* 45 (4) (2009) 299–304.
- [19] M. Keusgen et al., Development of a biosensor specific for cysteine sulfoxides, *Biosensors Bioelectronics* 18 (5–6) (2003) 805–812.
- [20] S. Huang et al., Spray drying of probiotics and other food-grade bacteria: A review, *Trends in Food Science & Technology* 63 (2017) 1–17.
- [21] O. Kašpar et al., Effect of cross-linking method on the activity of spray-dried chitosan microparticles with immobilized laccase, *Food and Bioprocess Processing* 91 (4) (2013) 525–533.
- [22] H.R. Costantino et al., Effect of mannitol crystallization on the stability and aerosol performance of a spray-dried pharmaceutical protein, recombinant humanized anti-IgE monoclonal antibody, *Journal of pharmaceutical sciences* 87 (11) (1998) 1406–1411.
- [23] Encapsulation of bioactive ingredients by spray drying, in *Spray Drying Techniques for Food Ingredient Encapsulation*, C. Anandharamakrishnan and S. Padma Ishwarya, Editors. p. 156-179.
- [24] B. Strehlow et al., A novel microparticulate formulation with alliin in situ synthesis, *J Pharm Drug Deliv Res* 5 1 (2016) 2.
- [25] L. Zhang et al., Maltodextrin: A consummate carrier for spray-drying of xylooligosaccharides, *Food Research International* 106 (2018) 383–393.
- [26] N.K. Mohammed et al., Spray drying for the encapsulation of oils—A review, *Molecules* 25 (17) (2020) 3873.
- [27] B.N. Estevinho et al., Microencapsulation with chitosan by spray drying for industry applications—A review, *Trends in food science & technology* 31 (2) (2013) 138–155.
- [28] Stoll, A., Seebeck, E., Allium compounds. III Specificity of alliinase and synthesis of compounds related to alliin. *Helvetica Chimica Acta*, 1949. 32: p. 866-868.
- [29] T. Mallika, E. Omer, Z. Lian-fu, Separation and Purification of Alliinase and Alliin from Garlic (*Allium sativum*), *Journal of Academia and Industrial Research* 2 (11) (2014) 599–605.
- [30] P. Janská et al., Effect of physicochemical parameters on the stability and activity of garlic alliinase and its use for in-situ alliin synthesis, *Plos one* 16 (3) (2021) e0248878.
- [31] Manabe, T., et al., Alliinase [S-alk (en) γ -L-cysteine sulfoxide lyase] from *Allium tuberosum* (Chinese chive) Purification, localization, cDNA cloning and heterologous functional expression. 1998. 257(1): p. 21-30.
- [32] N.J. Kruger, The Bradford method for protein quantitation, in: *The protein protocols handbook*, Springer, 2009, pp. 17–24.
- [33] M.M. Bradford, A rapid and sensitive method for the quantitation of microgram quantities of protein utilizing the principle of protein-dye binding, *Analytical Biochemistry* 72 (1) (1976) 248–254.

- [34] M.R.I. Shishir, W. Chen, Trends of spray drying: A critical review on drying of fruit and vegetable juices, *Trends in Food Science & Technology* 65 (2017) 49–67.
- [35] R.L. Carr, Evaluating flow properties of solids, *Chem. Eng.* 18 (1965) 163–168.
- [36] S.J. Compton, C.G. Jones, Mechanism of dye response and interference in the Bradford protein assay, *Analytical Biochemistry* 151 (2) (1985) 369–374.
- [37] A. Rabinkov et al., Alliin lyase (Alliinase) from garlic (*Allium sativum*). Biochemical characterization and cDNA cloning, *Applied biochemistry and biotechnology* 48 (3) (1994) 149–171.
- [38] Bergmeyer, H.U. and E. Bernt, UV-Assay with Pyruvate and NADH, in *Methods of Enzymatic Analysis* (Second Edition), H.U. Bergmeyer, Editor. 1974, Academic Press, p. 574–579.
- [39] Clark, D.S. and H.W. Blanch, *Biochemical engineering*. 1997: CRC press.
- [40] J. Wang et al., Effect of ultrasound on the activity of alliinase from fresh garlic, *Ultrasonics Sonochemistry* 18 (2) (2011) 534–540.
- [41] Y. Liu et al., The effect of ultrasound on lipase-catalyzed hydrolysis of soy oil in solvent-free system, *Ultrason Sonochem* 15 (4) (2008) 402–407.
- [42] D. Santos et al., *Spray Drying: An Overview*, *Biomaterials-Physics and Chemistry-New Edition* (2017).
- [43] M. Li, D. Wilkinson, K. Patchigolla, Comparison of Particle Size Distributions Measured Using Different Techniques, *Particulate Science and Technology* 23 (3) (2005) 265–284.
- [44] Scientific, H., Understanding and interpreting particle size distribution calculations. Downloaded Jun, 2018. 18.
- [45] O. Kašpar, M. Jakubec, F. Štěpánek, Characterization of spray dried chitosan-TPP microparticles formed by two- and three-fluid nozzles, *Powder Technology* 240 (2013) 31–40.
- [46] V. Tokárová et al., Development of spray-dried chitosan microcarriers for nanoparticle delivery, *Powder technology* 235 (2013) 797–805.
- [47] Don, W.G. and H.P. Robert, *Perry's Chemical Engineers' Handbook*, Eighth Edition. 8th ed. / ed. 2008, New York: McGraw-Hill Education.
- [48] J.F. Carpenter, L.M. Crowe, J.H. Crowe, Stabilization of phosphofructokinase with sugars during freeze-drying: characterization of enhanced protection in the presence of divalent cations, *Biochimica et Biophysica Acta (BBA) - General Subjects* 923 (1) (1987) 109–115.
- [49] M.J. Hageman, The role of moisture in protein stability, *Drug Development and Industrial Pharmacy* 14 (14) (1988) 2047–2070.
- [50] C. Dima et al., The kinetics of the swelling process and the release mechanisms of *Coriandrum sativum* L. essential oil from chitosan/alginate/inulin microcapsules, *Food Chemistry* 195 (2016) 39–48.
- [51] J. Siepman, N.A. Peppas, Modeling of drug release from delivery systems based on hydroxypropyl methylcellulose (HPMC), *Advanced Drug Delivery Reviews* 48 (2) (2001) 139–157.
- [52] Zetasizer Nano Series technical note MRK654-01, Malvern Instruments, UK, 2006.